Experimental evidence for an achiral orthogonal biaxial smectic phase without in-plane order exhibiting antiferroelectric switching behavior

A. Eremin, S. Diele, G. Pelzl, H. Nádasi, W. Weissflog, J. Salfetnikova, and H. Kresse
Institut für Physikalische Chemie, Martin-Luther-Universität, Halle-Wittenberg, Mühlpforte 1, D-06108 Halle (Saale), Germany
(Received 5 June 2001; published 22 October 2001)

We report unambiguous experimental evidence for an achiral orthogonal biaxial smectic-*A* phase which exhibits antiferroelectric switching behavior. The evidence is based on x-ray-diffraction measurements, texture observation, and the results of dielectric and electro-optical measurements.

DOI: 10.1103/PhysRevE.64.051707 PACS number(s): 61.30.Eb, 61.30.Cz, 61.30.Gd

I. INTRODUCTION

Conventional smectic phases, designated by the code letters Sm-*A* and Sm-*C*, are constituted by a stack of layers in which the molecules are aligned parallel (Sm-*A*) and obliquely (Sm-*C*) with respect to the layer normal. In the layers the lateral order is liquidlike. The Sm-*A* phase is optically uniaxial with the local symmetry $D_{\infty h}$; the Sm-*C* phase is biaxial with the local symmetry C_{2h}.

As was pointed out by de Gennes [1], a biaxial smectic phase may also appear if one of the principal axes of the magnetic susceptibility tensor $Q_{\alpha,\beta}$ is parallel to the layer normal but the transversal components of the tensor $Q_{\xi,\xi}$ and $Q_{\eta,\eta}$ are no longer equivalent. In this case, the molecules are aligned parallel to the layer normal but the properties with respect to the in-plane directions are different. This smectic phase was designated by the code letter C_M, where *M* refers to McMillan [2,3], who established the first microscopic theory of the Sm-*A* and Sm-*C* phase.

In a theoretical investigation done by Brand *et al.* [4], the inequivalence of the transversal components of *Q* has been achieved by considering boardlike molecules where for steric reasons $Q_{\xi,\xi} \neq Q_{\eta,\eta}$ and the phase possesses D_{2h} symmetry. Up to now, three liquid crystalline systems have been reported that exhibit a C_M phase [5–7].

Another way of obtaining $Q_{\xi,\xi} \neq Q_{\eta,\eta}$ might be found among the compounds with bent-core mesogens. The sterical moment caused by molecular geometry may provoke a polar packing within the layers, which causes a polarization in the bent direction [8–10]. If the alignment of the molecules is orthogonal with respect to the layer planes, a local C_{2v} symmetry results (in contrast to the C_M phase). This phase is similar to the Sm-*A* phase only in that one of the principal axes of *Q* is parallel to the layer normal.

It might be better to call it Sm-*AP* in analogy to the well-known tilted variant designated as Sm-*CP* [10]. However, in our paper we will follow the terminology proposed in [4] and label it *Cp*, emphasizing biaxiality of the phase. The tilted switchable phase Sm-*CP* or B_2 is well studied, nevertheless the *Cp* phase has not been reported before for low-molar bent-core mesogens. In our paper, we will give experimental evidence for the existence of such a *Cp* phase, which was theoretically predicted by Brand *et al.* [4,11].

II. EXPERIMENT

The substance under investigation is a new banana-shaped 4-cyano-resorcinol derivative fluorinated on the outer rings in position 3 (Fig. 1). By means of polarizing microscopy and differential calorimetry (DSC, Perkin Elmer), the following phase sequence has been determined:

$$\text{crystal} \quad \underset{[74.6]}{\overset{73\,^\circ\text{C}}{\longrightarrow}} \quad \text{Sm-}X \quad \underset{[1.2]}{\overset{145\,^\circ\text{C}}{\longrightarrow}} \quad \text{Sm-}A \quad \underset{[16.7]}{\overset{180\,^\circ\text{C}}{\longrightarrow}} \quad \text{isotropic.}$$

The numbers in brackets below the transition temperatures are the corresponding transition enthalpies in kJ/mol. In order to investigate the structure of the mesophases, *x*-ray-diffraction measurements have been carried out. Measurements on powderlike samples were performed using a Guinier film camera and a Guinier goniometer (Huber Diffraktionstechnik, GmbH). Oriented samples of the mesophases were obtained by very slow cooling of a drop of the compound from the isotropic liquid on a glass plate. At these conditions, the smectic layers could be oriented parallel to the substrate surface. The scattered radiation has been recorded using a two-dimensional (2D) detector (HI-Star, Siemens AG). The incident x-ray beam was parallel to the glass plate, which shadowed the lower part of the reciprocal sphere and an additional analysis was required to obtain the full picture.

The electro-optical measurements were carried out using commercial ITO cells (EHC). The spontaneous polarization was measured using the pulse as well as the triangular wave voltage method.

Dielectric measurements were performed in a double plate capacitor (area, 2 cm^2; spacing, 0.02 cm) using the HP 41192A and the Solartron Schlumberger SI 1260 impedance analyzer.

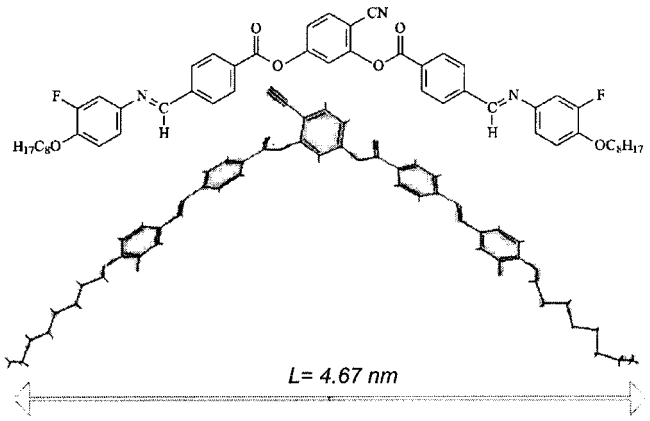

FIG. 1. Structural formula and simulated molecular conformation.

III. RESULTS

A. Optical and thermal behavior

Two mesophases could be clearly detected by calorimetry and polarizing microscopy. From the DSC thermogram one can see that the transition enthalpy between the two mesophases is quite low (1.2 kJ/mol) in comparison with the Sm-*A*-isotropic transition enthalpy (16.7 kJ/mol). The high-temperature mesophase exhibits a fan-shaped texture or a homeotropic texture indicating a Sm-*A* phase. On cooling, the fan-shaped texture remains nearly unchanged after the transition into the low-temperature phase. Only some irregular fine stripes parallel to the smectic layers appear on further cooling. However, if the Sm-*A* phase shows a homeotropic texture, it transforms into a strongly fluctuating schlieren texture (Fig. 2). On further cooling down to room temperature, the textures of the low-temperature phase are not markedly changed: the stripes in the fan-shaped texture slightly increase and the schlieren texture becomes more birefringent while the fluctuations completely disappear.

B. Dielectric properties

The dielectric permittivities have been obtained by fitting of the experimental data to the modified equation

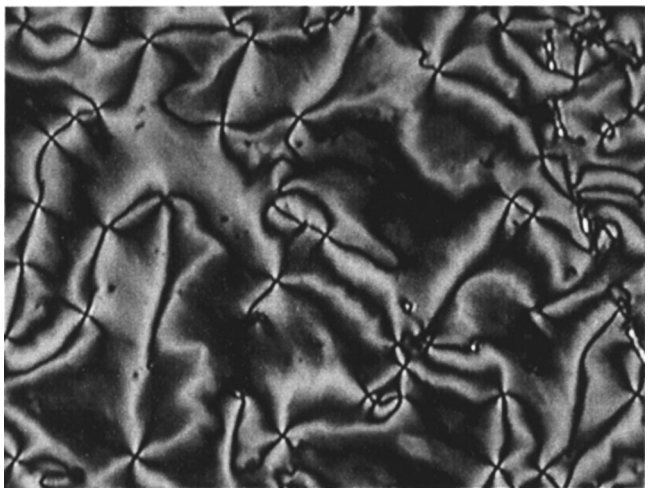

FIG. 2. Schlieren texture of the low-temperature phase.

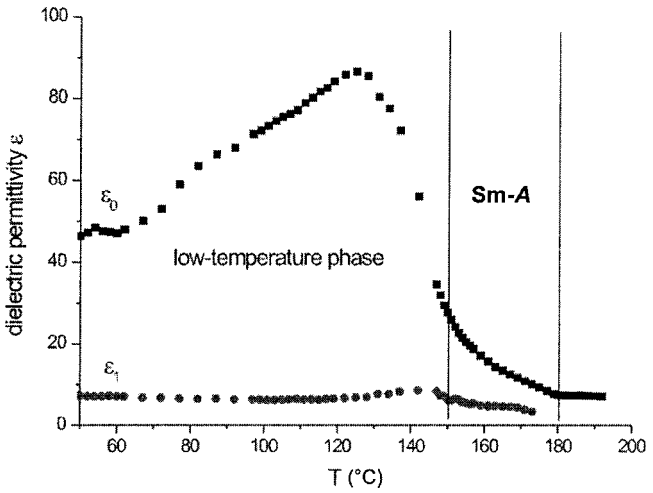

FIG. 3. Averaged dielectric permittivity (ε_0 and ε_1) as a function of the temperature.

$$\varepsilon^* = \varepsilon_1 + \frac{\varepsilon_0 - \varepsilon_1}{1 + (j\omega\tau_1)^{1-\alpha_1}} - \frac{jA}{f} + \frac{B}{f^N}, \tag{1}$$

which contains a Cole-Cole mechanism (terms 1 and 2, with ε_0 as the low- and ε_1 as the high-frequency limit of the dielectric constant, $\omega = 2\pi f$, f is the frequency, τ_1 is the relaxation time, and α_1 is the Cole-Cole distribution parameter), conductivity term 3 and term 4 which consider the capacitance of the double layer at the interface sample/gold electrode, and $\varepsilon^* = \varepsilon'(\omega) - i\varepsilon''(\omega)$ is the complex dielectric permittivity.

The limits of the dielectric permittivities obtained are shown in Fig. 3, and the related relaxation times are presented in Fig. 4. The molecular mechanism for this motion is the reorientation of the whole molecule about the long molecular axes [12]. A special low-frequency absorption found in many samples exhibiting the B_2 phase [13] could not be separated. This may be related to the high conductivity of the sample, which superimposes such a relaxation.

An interesting feature of the compound is the continuous increase of the static dielectric permittivity ε_0 with decreasing temperature from about 7 in the Sm-*A* phase up to 83 in the low-temperature phase. This behavior unambiguously indicates a pronounced dipole correlation in the low-temperature phase. For the time constant τ_1 only a change of

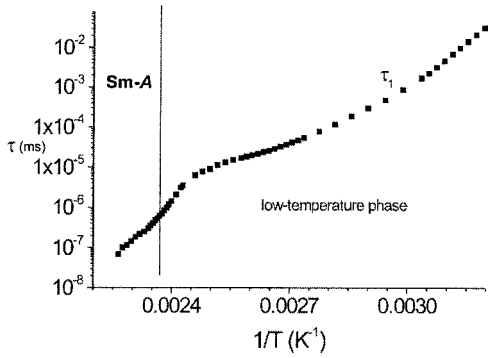

FIG. 4. Temperature dependence of the relaxation time τ_1.

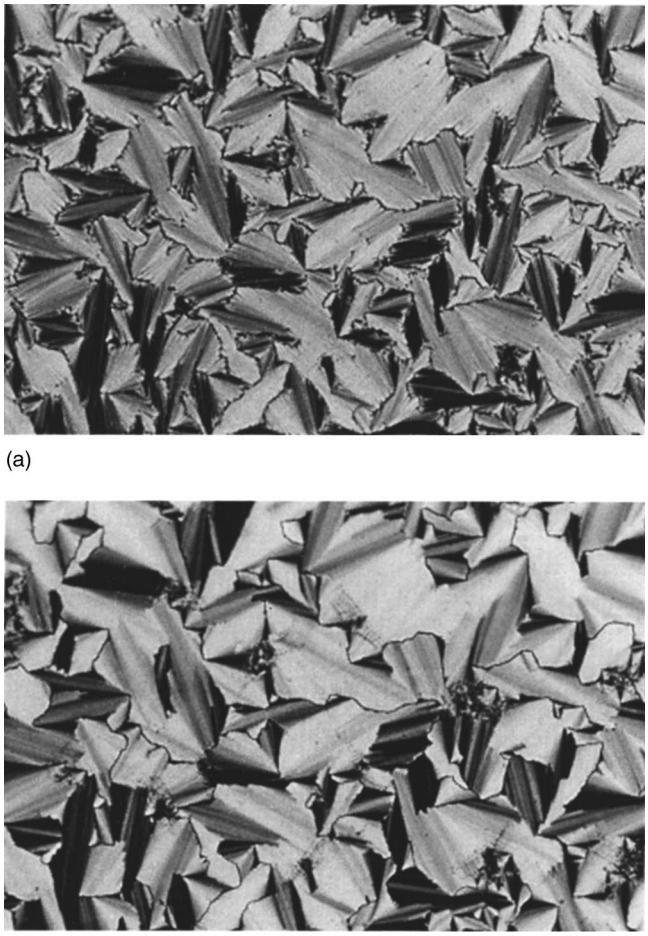

(a)

(b)

FIG. 5. Optical textures of the low-temperature phase: (a) 0 V μm^{-1}; (b) ± 8 V μm^{-1} (sample thickness: 10 μm; temperature: 138 °C).

the activation energy at the transition into the low-temperature phase is observed. An unexpectedly high value of $E_A = 200\,\mathrm{kJ\,mol^{-1}}$ of the Sm-*A* modification may result from the continuous change of the dipole correlation in this phase.

At room temperature an additional high-frequency absorption band was detected, characterized by the low- and high-frequency limits of the dielectric permittivity ε_1 and ε_2 as well as the time constant τ_2. This process is related to local motions, for example that of the terminal dipoles.

C. Electro-optical measurements

As is expected, the Sm-*A* phase does not show field-induced switching. Applying an electric field to the fan-shaped texture of the low-temperature phase, the birefringence (and therefore the interference color) is changed and the stripes within the fans disappear. Furthermore, the texture of the switched states is independent of the polarity of the applied field (Fig. 5). At lower temperatures (<60 °C), the field-induced switching is considerably delayed and takes some seconds. Two current peaks during a half-period of an applied triangular voltage give evidence for the antiferroelectric nature of this phase. The two-loop antiferroelectric hysteresis curve obtained by integration of the current response is shown in Fig. 6. The spontaneous polarization is plotted as a function of the temperature in Fig. 7. It is seen that the polarization is unusually high and reaches values of 1000 nC/cm^2. It is the highest value reported for banana-shaped mesogens so far. This high value is obviously a consequence of the high dipole correlation found in this phase.

D. X-ray studies

The x-ray diagram of the nonoriented samples displays the first three orders of the layer reflections as well as the diffuse outer scattering in a temperature range between 170 and 70 °C (Fig. 8). The positions of the quasi-Bragg reflections are nearly independent of the temperature, which means the layer thickness ($d = 4.43$ nm) remains constant within the limits of 0.02 nm. In the diagrams obtained from the oriented samples, also up to three on-the-meridian reflections are observed (Fig. 9, here the 001 reflection is covered by the beam stop). The x-ray-diffraction pattern exhibits an outer diffuse scattering, the maxima of which are clearly positioned on the equator, also in the phase below the Sm-*A* phase. No change in the patterns appears down to 45 °C, where the layer reflections become more crescentlike and the outer diffuse scattering splits into a few peaks resulting from the appearance of an in-plane order. But it is clearly seen that these wide-angle reflections still remain diffuse. The analysis

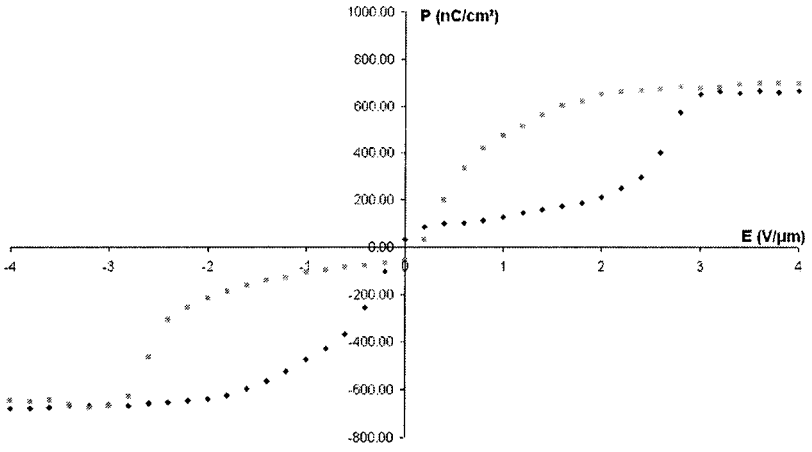

FIG. 6. Polarization plotted as a function of the electric field (138 °C).

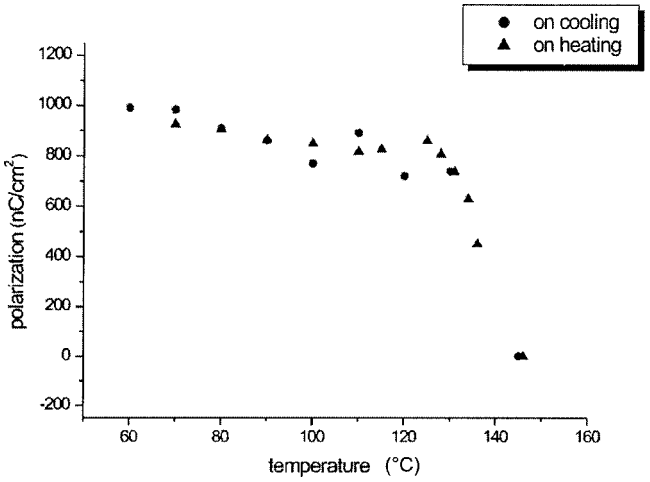

FIG. 7. Temperature dependence of the spontaneous polarization.

of the intensity of the diffuse outer scattering was performed with respect to the θ dependence (θ is the Bragg angle) as well as the χ dependence. The profile of the outer diffuse scattering $I(\theta)$ remains unchanged within the limits of error down to 100 °C. The experimental curves $I_{\mathrm{meas}}(\chi)$ were normalized with a transmission function $t(\chi)$, in order to prevent experimentally caused errors by shadowing the lower part of the reciprocal space. The transmission function $t(\chi)$ has been obtained by recording the scattering of the sample in the isotropic phase. In this ideal case, the intensity of the diffuse scattering is independent of χ. Then the corrected distribution of the scattering intensity in the mesophase is

$$I(\chi)=I_{\mathrm{meas}}(\chi)/t(\chi). \tag{2}$$

The function $I(\chi)$ is nearly identical in the Sm-*A* and in the low-temperature phase. The calibration allows us to determine the position of the maximum within the error of $\Delta\chi=\pm 1°$. The derived tilt angle ψ is outlined in Fig. 10. It is seen that in both smectic phases (Sm-*A* and the low-temperature phase), the molecules are aligned parallel to the layer normal.

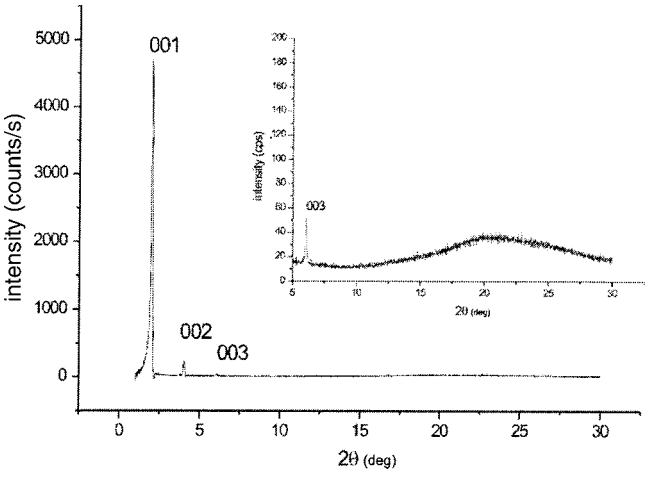

FIG. 8. X-ray diagram of a nonoriented sample.

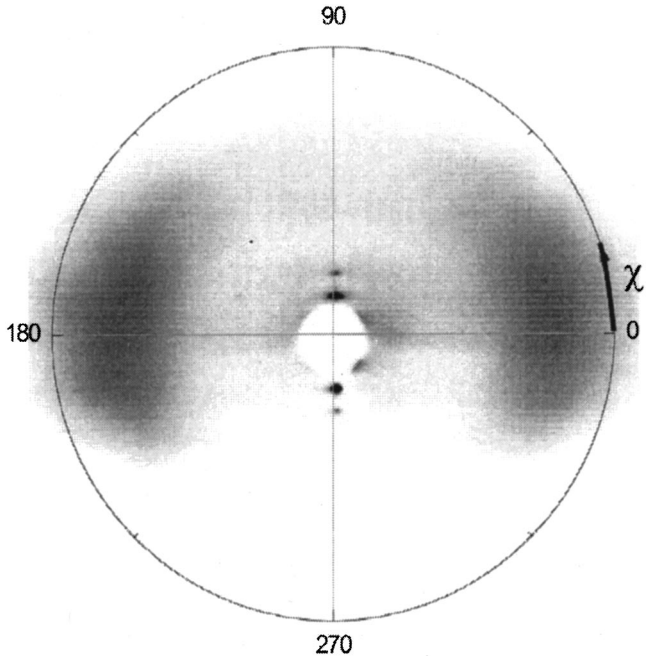

FIG. 9. X-ray pattern of an oriented sample.

E. Structure model

The structure model has been proposed on the basis of powder x-ray pattern simulation using CERIUS2 software and comparing it with the experimental data. In order to assign an initial conformation (corresponding to the minimal value of the free energy), the modeled molecule was subjected to the ''smart minimizer'' option of the simulation software, which uses ''universal force field'' [14] and includes the descent method, followed by the ABNR and quasi-Newton methods, and ending with the truncated Newton method. The minimization follows the standard scheme: the first minimization neglects the Coulomb term in the energy, then the charge equilibration scheme [15] is introduced, and the final minimization takes into account the electrostatic potential. This final conformation of the molecule was used to estimate the layer spacings and molecular form factor so as to simulate the powder pattern and then compare it with the experimental one.

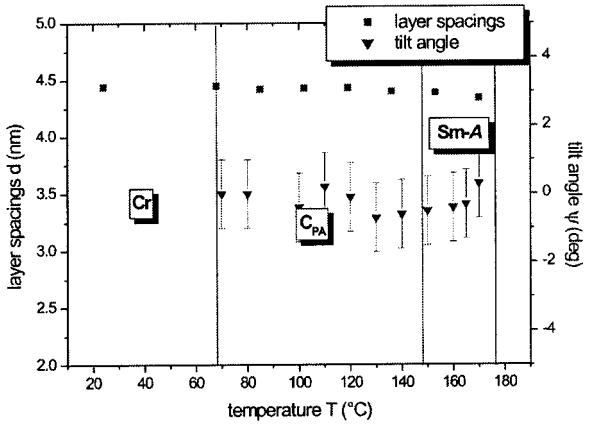

FIG. 10. Temperature dependence of the layer spacing *d* and the tilt angle ψ.

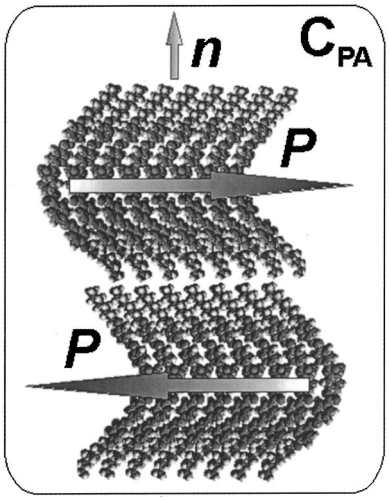

FIG. 11. Packing of the molecules in the low-temperature phase C_{PA}.

The results are as follows: (i) the bent angle is estimated to be around 106°, (ii) the molecular length $L=4.67\,\mathrm{nm}$.

Using the molecular shape shown in Fig. 1 and an orthogonal arrangement of the molecules within the layer, the structure factor was calculated and multiplied with a Debye-Waller factor ($\sigma=0.7\,\mathrm{nm}$). The calculated intensities of the three reflections ($00l$: $l=1-3$) agree well with the experimentally obtained ones. It leads to a packing shown in Fig. 11. However, it can still serve us only as a rough approximation since the minimization was performed without consideration of the surrounding of the molecule.

IV. DISCUSSION

Summarizing the experimental results, we can see that the low-temperature phase is a smectic phase without in-plane order and with an orthogonal alignment of the molecules, which resembles the Sm-A phase. But in contrast to Sm-A, this phase does not form a homeotropic texture but rather a schlieren texture, which mainly displays defects of the strength ± 1 (sometimes also $\pm\frac{1}{2}$). At first sight these findings are compatible with a C_M phase. However, the antiferroelectric switching observed on this compound indicates the presence of the polar axis, which reduces the symmetry of the phase to C_{2v} (different from D_{2h} of the C_M phase). From these results we can conclude that the low-temperature phase is an antiferroelectric version of the C_P phase discussed by Brand *et al.* [4,11] and designated as a C_{PA} phase. In this smectic phase, the banana-shaped molecules are packed in the bent direction, which is identical with the polar axis. The smectic layers have C_{2v} symmetry, i.e., a twofold symmetry axis (which coincides with the polar axis) and a vertical mirror plane including the twofold axis and the layer normal. In addition, the polar direction alternates from layer to layer giving rise to the antiferroelectric structure of the C_{PA} phase. This is suggested by the sporadic occurrence of $s=\pm\frac{1}{2}$ defects in the schlieren texture, which cannot be formed in the ferroelectric C_P phase. It is known that in smectic phases where the tilt of the molecules or of the mesogenic units alternates in adjacent layers, i.e., in Sm-C_A phases or in intercalated Sm-C phases [16–18], $s=\frac{1}{2}$ defects can arise by a combination of a disclination and a screw dislocation (dispiration). The same should be true for the C_{PA} phase under discussion.

Further on, in the C_P or C_{PA} phase, chiral smectic layers cannot exist like in the B_2 phase of banana-shaped compounds, where the bent-shaped molecules are tilted with respect to the layer normal [10]. Therefore, racemic or homogeneously chiral domains cannot be observed in C_P and C_{PA} phases.

It should be noted that in mixtures of a side-chain polymer and its monomer, a smectic phase with alternating tilt of the mesogenic unit is described [19]. In pyroelectric experiments, this phase shows antiferroelectric properties, but a field-induced switching could not be observed. Although the structure of this phase is clearly different from that of the C_{PA} phase presented here, the symmetry and the antiferroelectric nature of this phase seem to be the same.

ACKNOWLEDGMENTS

This work was supported by the Deutsche Forschungsgemeinschaft (DFG) and the Fonds der Chemischen Industrie.

[1] P. G. de Gennes, *The Physics of Liquid Crystals* (Clarendon, Oxford, 1974).
[2] W. L. McMillan, Phys. Rev. A **4**, 1238 (1971).
[3] W. L. McMillan, Phys. Rev. A **8**, 1921 (1973).
[4] H. R. Brand, P. E. Cladis, and H. Pleiner, Macromolecules **25**, 7223 (1992).
[5] H. F. Leube and H. Finkelmann, Makromol. Chem. **192**, 1317 (1991).
[6] R. Pratibha, N. V. Madhusudana, and B. K. Sadashiva, Science **288**, 2184 (2000).
[7] T. Hegmann, J. Kain, S. Diele, G. Pelzl, and C. Tschierske, Angew. Chem. **113**, 911 (2001).
[8] T. Niori, T. Sekine, J. Watanabe, and H. Takezoe, J. Mater. Chem. **6**, 1231 (1996).
[9] G. Pelzl, S. Diele, and W. Weissflog, Adv. Mater. **11**, 707 (1999).
[10] D. R. Link, G. Natale, R. Shao, J. E. Maclennan, N. A. Clark, E. Körblova, and D. M. Walba, Science **278**, 1924 (1997).
[11] H. R. Brand, P. E. Cladis, and H. Pleiner, Eur. Phys. J. B **6**, 347 (1998).
[12] G. Pelzl, S. Diele, S. Grande, A. Jakli, Ch. Lischka, H. Kresse, H. Schmalfuss, I. Wirth, and W. Weissflog, Liq. Cryst. **26**, 401 (1999).
[13] H. Schmalfuss, A. Hauser, and H. Kresse, Mol. Cryst. Liq. Cryst. Sci. Technol., Sect. A **351**, 221 (2000).
[14] A. K. Rappe *et al.*, J. Am. Chem. Soc. **114**, 10 024 (1992).
[15] A. K. Rappe *et al.*, J. Phys. Chem. **95**, 3358 (1991).

[16] W. F. Harris, Philos. Mag. **22**, 949 (1970).
[17] Y. Takanishi, H. Takezoe, A. Fukuda, and J. Watanabe, Phys. Rev. B **45**, 7684 (1992).
[18] W. Weissflog, S. Richter, E. Dietzmann, J. Risse, S. Diele, P. Schiller, and G. Pelzl, Cryst. Res. Technol. **32**, 271 (1997).
[19] E. A. Soto Bustamente, S. V. Yablonskii, B. I. Ostrovskii, L. A. Beresnev, L. M. Blinov, and W. Haase, Chem. Phys. Lett. **260**, 447 (1996); Liq. Cryst. **21**, 829 (1996).